RSC Advances

ROYAL SOCIETY OF CHEMISTRY

www.rsc.org/advances

Unusual magnetic response in π-stacked 6^6-dia net structure of [4+2] copper(II) cubane

Mithun Das,[‡,a] Bikash Kumar Shaw,[‡,b] Biswa Nath Ghosh,[c] Kari Rissanen,[c] Shyamal Kumar Saha[*,b] and Shouvik Chattopadhyay[*,a]

Abstract

A phenoxo bridged antiferromagnetic copper(II) cubane, features a π-stacked 6^6-**dia** net framework, which creates long range ferromagnetic ordering, as evidenced from a coercivity maximum (~2000 Oe) at 20K with very unusual saturation magnetization.

Keywords: copper(II); [4+2] cubane; π-stacked 6^6-**dia** net; long range ferromagnetic ordering; coercivity

High-nuclearity transition metal complexes have attracted much attention because of their unusual physical properties[1] and relevance to biological function in metalloproteins.[2] Among them, oxygen bridged tetrameric copper(II) clusters having Cu_4O_4 cubane cores have been extensively studied in order to provide clear insight into the relationship between their structural features and the strength of the magnetic exchange interaction between the copper(II). It is now well established that the exchange coupling of phenoxo bridged polynuclear copper(II) complexes depends on various structural features such as the coordination geometry of the copper(II), Cu−O(R)−Cu angles, Cu−O bond lengths, Cu···Cu distances etc.[3] The copper(II) cubanes may have six equivalent Cu···Cu distances, two short and four long Cu···Cu distances or four short and two long Cu···Cu distances.[4] Although, there are several reports on the correlations between the structural parameters and magnetic properties for oxygen bridged copper(II) cubanes,[5] the consequence of long range ferromagnetic ordering is not explored. The long range ferromagnetic ordering could be achieved by strong inter-cubane coupling and several

strategies could be developed to increase the inter-cubane coupling, such as the creation of hydrogen bonding and π···π stacking among neighbouring cubanes. The importance of hydrogen bonding in propagating the magnetic interactions among the metal centers of neighboring molecules was reported in literature.[6] The supramolecular H-bonding interaction intervenes the ferromagnetic super-exchange coupling in the dinuclear assemblies. These works shows that Water molecules, carboxylate bridges and even the nitrate ion mediate the exchange coupling between the metal centers. 18-crown-6 also participates in the exchange processes through H-bonding interactions. Even the magnetic interaction between metal centers connected through aromatic moieties via strong π···π stacking was shown to depend upon the stacking angle and interaction between the spin densities of the stacked layers.[7] However, best to our knowledge, there is no report regarding the long range ferromagnetic ordering in copper(II) cubanes connected through strong π···π stacking.

We have used a semicarbazone Schiff base, HL, to prepare a phenoxo bridged copper(II) cubane, $[Cu_4(L)_4](ClO_4)_4 \cdot 4H_2O$ (Scheme S1, ESI). The complex features supramolecular 6^6-**dia** net framework and cyclic perchlorate–water octameric clusters in its solid state structure. Variable temperature magnetic susceptibility measurements showed that the copper(II) spins in the cubane core are antiferromagnetically coupled and the uncompensated spins of the adjacent cubane cores are ferromagnetically coupled through π···π stacking.

All starting materials were commercially available, reagent grade, and used as purchased from Sigma-Aldrich without further purification. **Caution!!!** Although no problems were encountered in this work, perchlorate salts containing organic ligands are potentially explosive. Only a small amount of the material should be prepared and they should be handled with care.

A methanol solution (20 ml) of semicarbazide hydrochloride (1 mmol, 120 mg) and 3-methoxysalicylaldehyde (1 mmol, 150 mg) were refluxed for ca. 1 h to produce the ligand 3-methoxysalicylaldehydesemicarbazone (HL). The ligand was not isolated. A methanol solution (10 ml) of copper(II) perchlorate hexahydrate (1 mmol, 370 mg) was added to it with constant stirring. The stirring was continued for additional 2 h. The resulting green solution was allowed to stand at room temperature. Single crystals, suitable for X-ray diffraction, started to separate from the resulting solution and was collected by filtration after ca. 2 days.

The complex crystallizes in tetragonal space group $I4_1/a$. The asymmetric unit consists of a cationic copper(II) complex, $[Cu(L)]^+$, one perchlorate anion and a water of crystallization (Figure 1A). Such four cationic units assembled together to form μ_3-phenoxo bridged cubane (Figure 1B). Within the cubane unit, Cu(1)···Cu(1)†, Cu(1)···Cu(1)$^{\diamond}$, Cu(1)†···Cu(1)* and Cu(1)$^{\diamond}$···Cu(1)* distances are significantly shorter (3.281 Å) compared to Cu(1)···Cu(1)* and Cu(1)†···Cu(1)$^{\diamond}$ distances (3.410 Å) († = -1/4+x,3/4-y, 7/4-z; * = 1-x,1/2-y,z and $^{\diamond}$ = 3/4-x,1/4+y,7/4-z). Thus the complex may be classified as a cubane with two short and four long Cu···Cu distances.[4] Selected bond angles (°) around copper(II) is shown in Table S1 (ESI). Each copper(II) in the cubane resides in identical environment. Cu(1) is coordinated by two oxygen atoms, O(1) and O(3), and one nitreogen atom, N(1), of the deprotonated ligand $(L)^-$ and two oxygen atoms, O(1)†, O(2)† of a symmetry related $(L)^-$. The sixth coordination site is occupied by an oxygen atom O(1)* from another symmetry related $(L)^-$. There are six Cu_2O_2 faces in the cubane, of which four Cu_2O_2 faces have two different Cu–O–Cu bridging angles {88.3° and 112.8° (β)} with three short (two 1.988 Å (d_1) and one 1.951 Å) and one long (d_2 ~2.672 Å) Cu–O bond lengths (Figure S1, ESI). The other two Cu_2O_2 faces have similar Cu–O–Cu bridging angles {93.7°(α)} with two short (~1.951 Å) and two long (d_2 ~2.672 Å) Cu–O bond lengths. The out of plane shift of the carbon atoms linked to bridged oxygen atoms makes the angle (τ) around 49.5°. The Cu–N bond distance (1.938 Å) is found to be shorter than the Cu–O bond distances (1.951–2.672 Å).

A cyclic perchlorate-water octameric $\boldsymbol{R_8^8}(16)$ ring has been produced by hydrogen bonding interactions among the lattice water molecules and perchlorate ions (Figure S2, ESI). This perchlorate-water octamer is hydrogen bonded with the cubane structure to form a three dimensional architecture (Figure S3, ESI). The details of hydrogen bonding interactions are given in ESI. The phenyl ring $\mathbf{R^{24}}$ [C(1)–C(2)–C(3)–C(4)–C(5)–C(6)] present within $[Cu(L)]^+$ unit shows π···π stacking with symmetry related (3/2-x,1/2-y,3/2-z) phenyl ring $\mathbf{R^{24}}$ (Table S2, ESI) and each cubane behaves like a tetrahedron vertex of a self assembled 6^6-**dia** net structure (Figure 2).[8]

The temperature dependence of the magnetic susceptibility (χ) (ZFC-FC) for the complex measured in the temperature range between 2 to 300 K is shown in Figure 3A. The ZFC-FC curves indicate a higher ordering temperature at around 300K. From the least squares analysis

(Figure S4), a strong antiferromagnetic exchange interaction is found between the bridged copper(II) centers with J = –40.8 cm^{-1} and a relatively weaker one with J′ = –4.9 cm^{-1} between the unbridged copper(II) centers respectively. (Details are given in ESI)

The most interesting feature in the magnetic properties of this intracluster antiferromagnetic structure is the observation of complicated hysteresis loops which show marked changes under application of thermal energy as shown in Figure S5 (ESI). Unlike other ferromagnetic materials, here, the hysteresis loops become wider as the temperature rises from 2K to 20K. Above 20K, a gradual decrease in coercive field is observed with a minimum of 160 Oe at 300K, which is in close agreement with ZFC-FC behavior. The variation of coercivities with temperature is summarized in Table S3 (ESI). At lower temperatures up to 10 K, magnetization becomes paramagnetic at higher field region due to unsaturation. The observation of highest coercivity at 20 K with clear saturation in magnetization is very unusual in this antiferromagnetic cubane structure (Figure 3B). This behavior clearly reveals a certain phase transition operated at lower temperatures.

To confirm the presence of magnetic phase, ac magnetic susceptibility measurements were carried out as a function of temperature. The measurements were performed at an applied dc field of 5 Oe and ac field of 3 Oe oscillating in the frequency range from 1.1–21.1 Hz. The relaxation peak, signifying the existence of magnetic phase is appeared both in real (χ') and imaginary (χ'') parts of susceptibility (Figure 3C,D).[9]

The unusual magnetic property could be explained with the help of supramolecular π···π stacking which vary with thermal energy. In our previous work, we have reported the enhancement of ferromagnetic ordering under the application of thermal energy.[10] In case of ferromagnetism that originated due to interaction between the S = ½ spins of metal centers via π···π stacking increases as a result of increase in overlapping area of the aromatic π-stacked moieties due to the strain generated in the crystal lattice resulting better ferromagnetic ordering at high temperature. The perfect overlapping of the aromatic π-stacked moieties results long range ferromagnetic interaction through the antiferromagnetic cubane cores. To explain the observed unusual ferromagnetic hysteresis loops we have considered the model schematically shown in Figure 4.

In this case, the copper(II) spins in the cubane core are antiferromagnetically coupled while the uncompensated spins of the adjacent cubane cores are ferromagnetically coupled through π···π stacking between the ligands. Basically, the magnitude of the uncompensated spin moment in the cubane core is smaller at 2K as the antiferromagnetic singlet state predominates at lower temperatures. However, at higher temperatures, the magnitude of the uncompensated spin moment increases in the antiferromagnetic core due to splintering of the coupled spins at higher temperature. At the same time, with increase in temperature overlapping between the π-stacked moieties increases upto 20K. This creates a path for the uncompensated spins to be coupled ferromagnetically in a long range manner, showing maximum ferromagnetic ordering at 20K. After 20K, the ferromagnetic ordering gradually decreases with a minimum coercivity of 160 Oe at temperature 300K, similar to a high temperature ferromagnet. Another point to be noted is the appearance of asymmetry in the hysteresis loop near the zero field region and the unsaturation in magnetization at high field region particularly for lower temperatures. This is correlated with the rise in magnetization below 20 K in the susceptibility data. The inverse of susceptibility (Figure S6) does not show linearity at low temperature which indicates that it does not follow Curie paramagnetism at all. This also implies that the rise in magnetization at low temperature is not due to paramagnetic impurities rather the uncompensated spin moment arises in the exchange process into the cubane core resulting the anomaly. The asymmetry (sharp fall of magnetization near zero field) arises due to antiferromagnetic coupling between the copper(II) spins in the cubane core. The exchange bias originated due to sequence of alternate ferromagnetic and antiferromagnetic exchange interactions causes the asymmetry in the coercivity as observed the highest value at 30 K.

In conclusion, a phenoxo bridged antiferromagnetic copper(II) cubane, $[Cu_4(L)_4](ClO_4)_4 \cdot 4H_2O$ forms 6^6-**dia** net supra-molecular framework via π···π stacking which, in turn, is responsible for a long range ferromagnetic ordering of the uncompensated spins of the adjacent cubane cores. The coercivity unusually increases with temperature. The origin of asymmetry in the hysteresis curve is the appearance of alternate antiferromagnetic and ferromagnetic interactions in the complex.

Acknowledgements

S.C. acknowledges DST, India under FAST Track Scheme (Order No. SR/FT/CS-118/2010, dated 15/02/2012). S.K.S. acknowledges DST, India (project No. SR/NM/NS-1089/2011) for providing facilities of magnetic measurements.

Notes and references

[a] Department of Chemistry, Inorganic Section, Jadavpur University, Kolkata 700032, India.

E-mail: shouvik.chem@gmail.com

[b] Department of Materials Science, Indian Association for the Cultivation of Science, Kolkata 700032, India. E-mail: cnssks@iacs.res.in

[c] Department of Chemistry, Nanoscience Center, University of Jyväskylä, P.O. Box 35, 40014 Jyväskylä, Finland.

‡ These authors contributed equally to this work.

Electronic supplementary information (ESI) available: Experimental details, Crystal data collection and refinement details, IR and electronic spectra, Photophysical and powder XRD study, Hydrogen bonding interactions and magnetic property.

Yield: 270 mg, 69%, based on copper(II). Anal. Calc. for $C_{36}H_{48}Cu_4N_{12}O_{32}Cl_4$ (1556.82): C, 27.77; H, 3.11; N, 10.80. Found: C, 27.9; H, 3.4; N, 10.6%. IR (cm^{-1}): 3426 (OH), 3381, 3298 (NH_2); 1642 (C=N), 1088 (Cl–O). UV–Vis, λ_{max} (nm) [ε_{max}(L mol^{-1} cm^{-1})] (acetonitrile): 627 (229), 498 (534), 375 (7131).

Crystal data: formula = $C_{36}H_{48}Cu_4N_{12}O_{32}Cl_4$, formula weight = 1556.82, crystal size (mm) = 0.14 x 0.19 x 0.29, temperature (K) = 173, crystal system = Tetragonal, space group = $I4_1/a$, a = 19.0353(6) Å, b = 19.0353(6) Å, c = 15.4705(7) Å, d_{calc} (gcm^{-3}) = 1.845, μ (mm^{-1}) = 1.795, F(000) = 3152, total reflections = 5120, unique reflections = 2604, observed data [$I > 2\sigma(I)$] = 2049, R(int) = 0.019, R1, wR2 (all data) = 0.0681, 0.1446, R1, wR2 [$I > 2\sigma(I)$] = 0.0502, 0.1274.

1. (a) Z.-H. Wei, C.-Y. Ni, H.-X. Li, Z.-G. Ren, Z.-R. Sun and J.-P. Lang, *Chem. Commun.*, 2013, **49**, 4836-4838; (b) G. Novitchi, W. Wernsdorfer, L. F. Chibotaru, J.-P. Costes, C. E. Anson and A. K. Powell, *Angew. Chem. Int. Ed.*, 2009, **48**, 1614–1619; (c) R. Saha, B. Joarder, A. S. Roy, S. M. Islam and S. Kumar, *Chem. Eur. J.*, 2013, **19**, 16607–16614.

2. (a) R. Than, A. A. Feldmann and B. Krebs, *Coord. Chem. Rev.*, 1999, **182**, 211-241; (b) Jr. L. Que and W. B. Tolman, *Angew. Chem. Int. Ed.*, 2002, **41**, 1114-1137.

3. (a) J.-P. Costes, C. Duhayon and L. Vendier, *Inorg. Chem.*, 2014, **53**, 2181−2187; (b) C. J. Calzado, *Chem. Eur. J.*, 2013, **19**, 1254–1261.

4. (a) E. Ruiz, A. Rodriguez-Fortea, P. Alemany and S. Alvarez, *Polyhedron*, 2001, **20**, 1323−1327; (b) E. Ruiz, P. Alemany, S. Alvarez and J. Cano, *J. Am. Chem. Soc.*, 1997, **119**, 1297−1303.

5. (a) D. Maity, A. D. Jana, M. Debnath, N. G. R. Hearns, M.-H. Sie, H. M. Lee, R. Clérac and M. Ali, *Eur. J. Inorg. Chem.*, 2010, 3484–3490; (b) J. Tercero, E. Ruiz, S. Alvarez, A. Rodriguez-Fortea and P. Alemany, *J. Mater. Chem.* 2006, **16**, 2729−2735.

6. (a) M. Zeng, W. Zhang, X. Sun and X. Chen, *Angew. Chem., Int. Ed.*, 2005, **44**, 3079–3082; (b) H. Miyasaka, H. Okawa, A. Miyazaki and T. Enoki, *Inorg. Chem.*, 1998, **37**, 4878-4883. (c) F. Yoe, M. Flores-Alamo, F. Morales, R. Escudero, H. Cortes-Hernandez, M. Castro and N. Barba-Behrens, *Inorg. Chim. Acta*, 2014, **423**, 36–45. (d) A. Drljaca, D. C. R. Hockless, B. Moubaraki, K. S. Murray and L. Spiccia, *Inorg. Chem.*, 1997, **36**, 1988-1989; (e) R.P. Doyle, M.Julve, F. Lloret, M. Nieuwenhuyzen and P. E. Kruger, *Dalton Trans.*, 2006, 2081–2088. (f) J. S. Costa, N. A. G. Bandeira, B. Le Guennic, V. Robert, P. Gamez, G. Chastanet, L. Ortiz-Frade, and L. Gasque, *Inorg. Chem*. 2011, **50**, 5696–5705.

7. (a) K. Yoshizawa and R. Hoffmann, *J. Am. Chem. Soc.*, 1995, **117**, 6921-6926; (b) L. Li, K. Lin, C. Ho, C. Sun and H. Yang, *Chem. Commun.*, 2006, 1286–1288; (c) Y. Zheng, M. Tong, W. Xue, W. Zhang, X. Chen, F. Grandjean and G. Long, *Angew. Chem.*, 2007, **119**, 6188–6192; (d) V. Lageta, C. Hornic, P. Rabu, M. Drillon and R. Ziessel, *Coord. Chem. Rev.*, 1998, **178–180**, 1533–1553.

8. (a) M. Scudder and I.Dance, *CrystEngComm*, 2001, 12, 1-4; (b) Z.-L. Wang, W.-H. Fanga and G.-Y. Yang, *Chem. Commun.*, 2010, **46**, 8216–8218.

9. N. Motokawa, H. Miyasaka, M. Yamashita and K. R. Dunbar, *Angew. Chem. Int. Ed.*, 2008, **47**, 7760 –7763.

10. S. Giri and S. K. Saha, *J. Phys. Chem. Lett.*, 2011, **2**, 1567–1572.

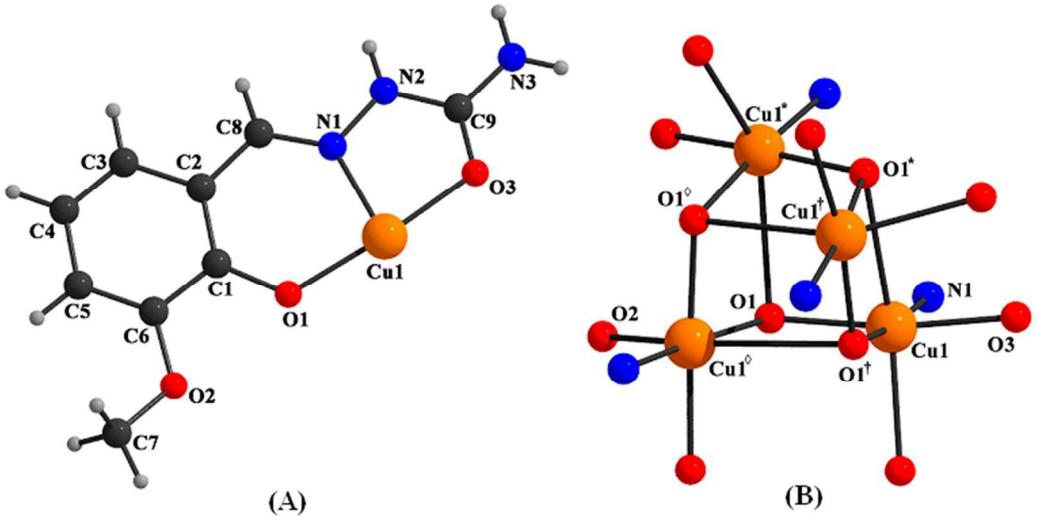

Figure 1: Perspective view of (A) $[CuL]^{+}$ unit and (B) Cu_4O_4 core of the complex. Selected bond lengths: Cu(1)-O(1) = 1.951(4), Cu(1)-O(3) = 1.956(4), Cu(1)-$O(1)^{*}$ = 2.672(4), Cu(1)-$O(1)^{\dagger}$ = 1.988(3), Cu(1)-$O(2)^{\dagger}$ = 2.244(4), Cu(1)-N(1) = 1.938(5).

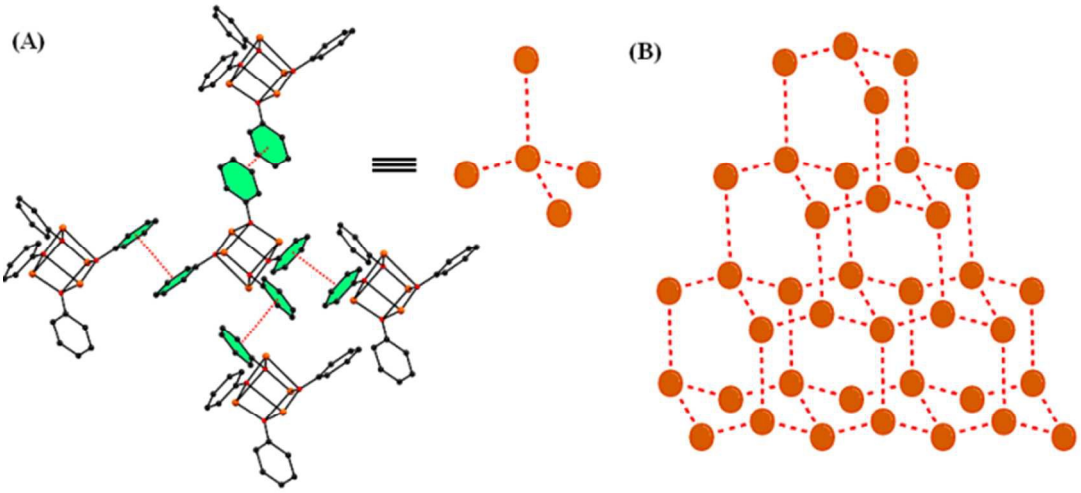

Figure 2: (A) π···π stacking between cubane units and (B) π-stacked 6^6-**dia** net structure of the complex.

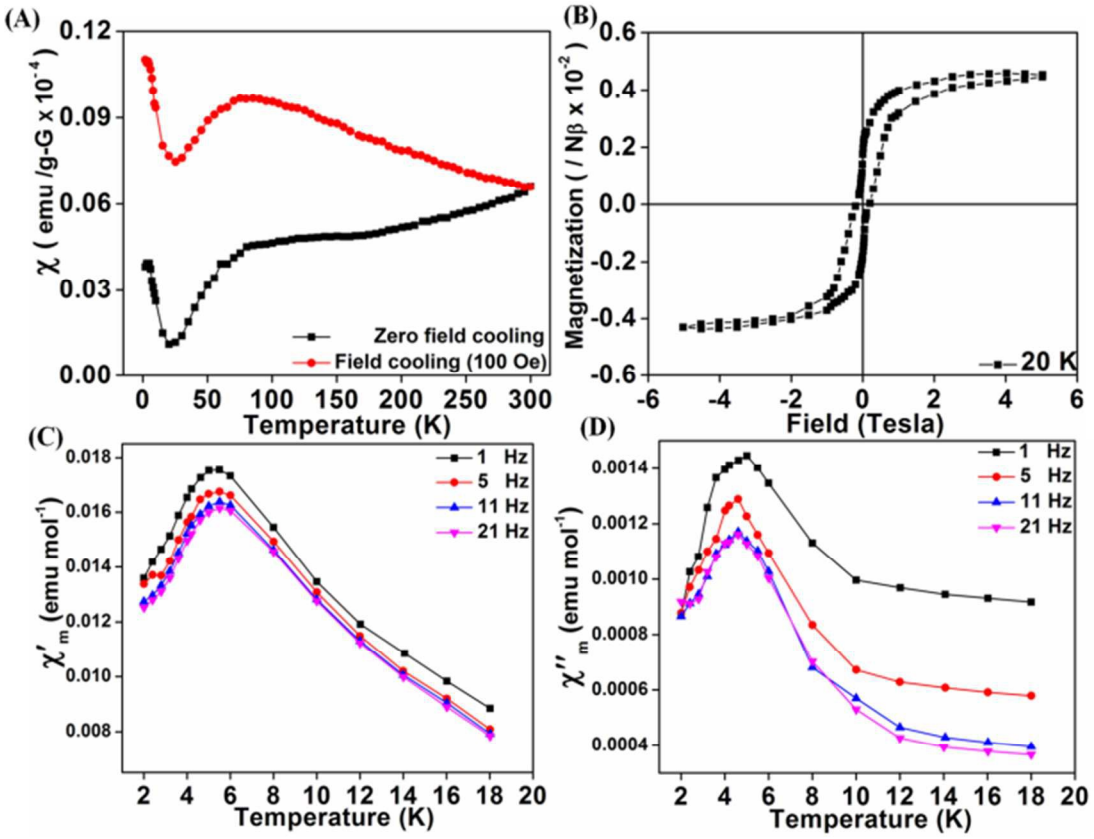

Figure 3: (A) Change in dc susceptibility (χ) values with temperature for the zero field cooling and field cooling processes measured at 100 Oe. (B) Variation of magnetization vs. magnetic field at 20K. In-phase (χ') (C) and out-of-phase (χ'') (D) AC susceptibilities at 5 Oe dc field and 3 Oe ac oscillating field.

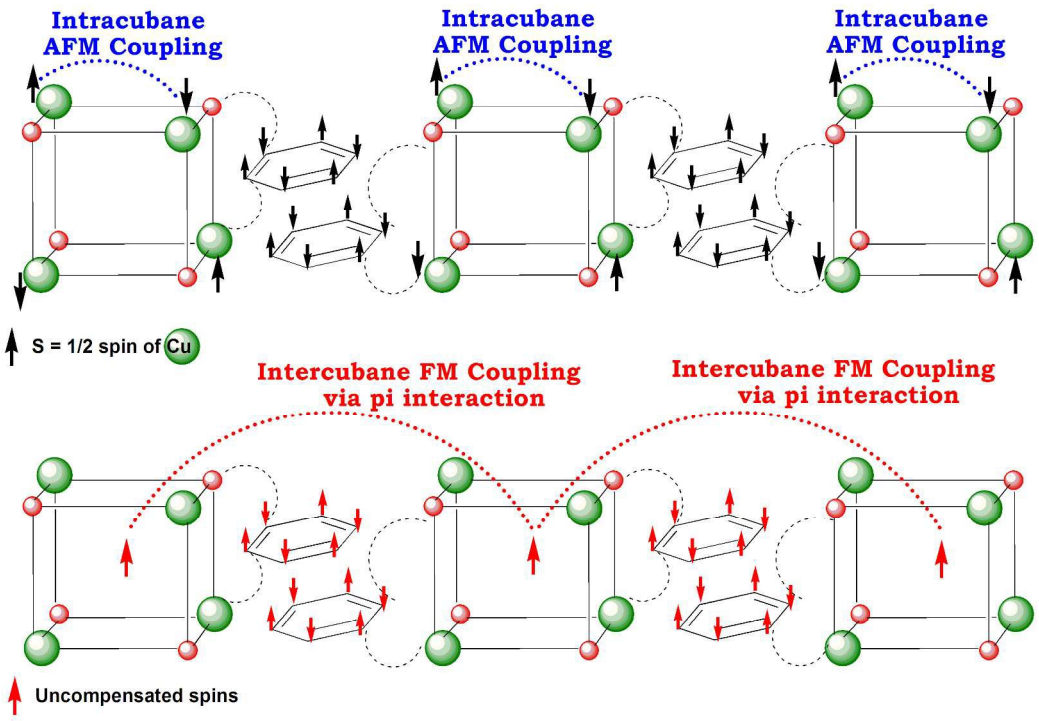

Figure 4: Schematic representation of antiferromagnetic exchange coupling between bridged copper atoms in the intracubane core (above) and intercubane long range ferromagnetic ordering mediated through π···π stacking (below)